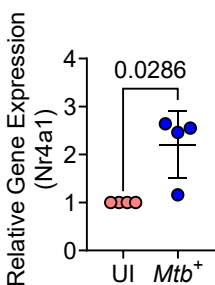
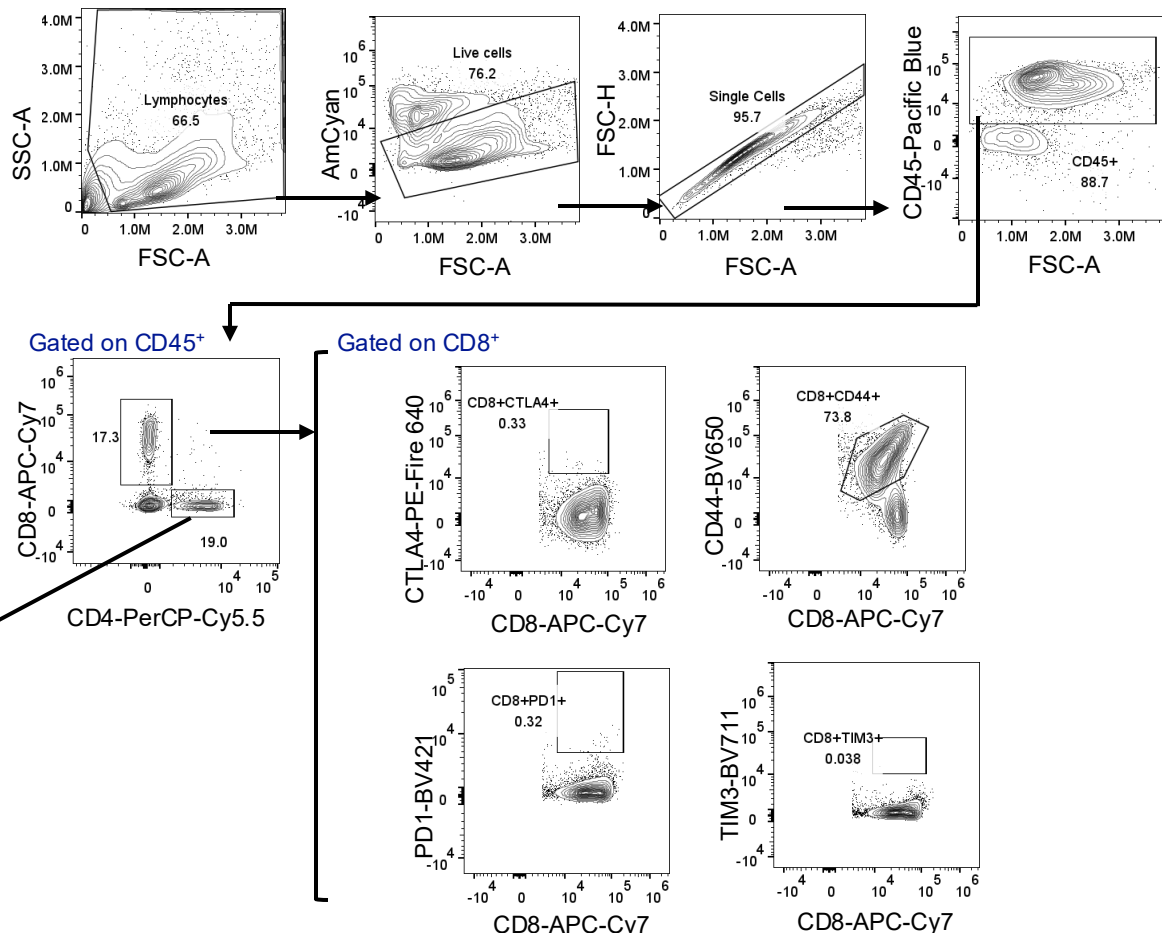
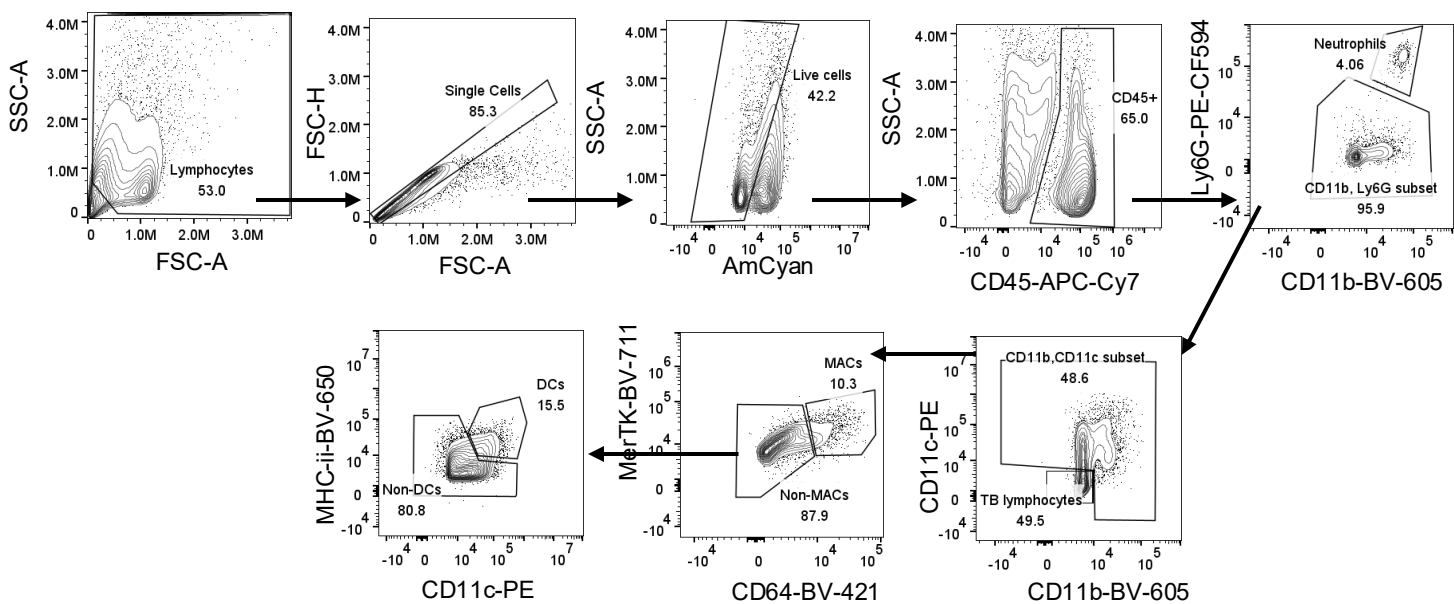
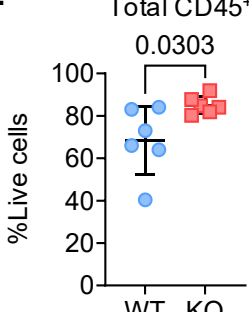
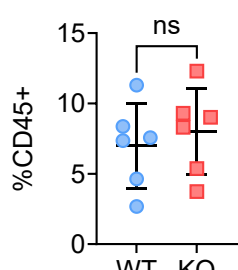
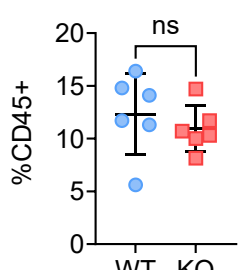
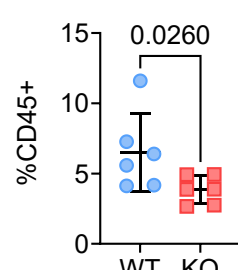
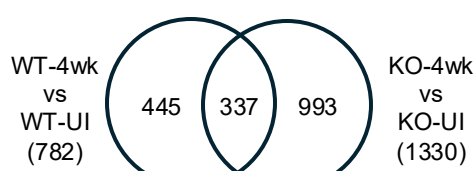


**a.****b.****c.****d.****e. Macrophages****f. Dendritic cells****g. Neutrophils**

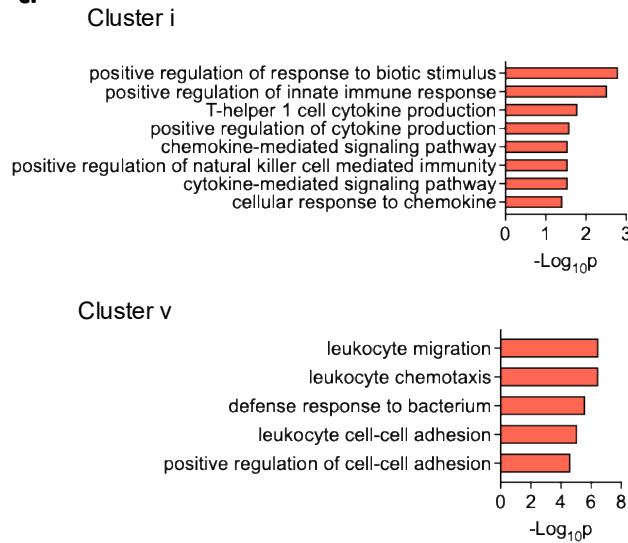
**Extended Data Fig. 1 Flow-cytometric gating and quantification of T cell and myeloid subsets in *Nr4a1*-deficient versus WT mice lungs.**

**a**, Lung *Nr4a1* mRNA levels in uninfected (UI) and *Mtb*-infected mice, shown as relative expression (qPCR). *P* value, two-tailed Mann–Whitney. Each dot represents one mouse. Data is mean  $\pm$  s.d. **b**, Flow cytometry gating for lung T cells using activation and exhaustion markers. **c**, Gating strategy for analyzing myeloid cells in the lung. **d**, Percentage of CD45 $^{+}$  T cells among live lung cells in WT and *Nr4a1* $^{-/-}$  mice. **e–g**, Macrophages (**e**), dendritic cells (**f**) and neutrophils (**g**) as a percentage of CD45 $^{+}$  lung leukocytes. Each dot is a mouse; horizontal bar indicates mean  $\pm$  s.d. *P* value, two-tailed Mann–Whitney test.

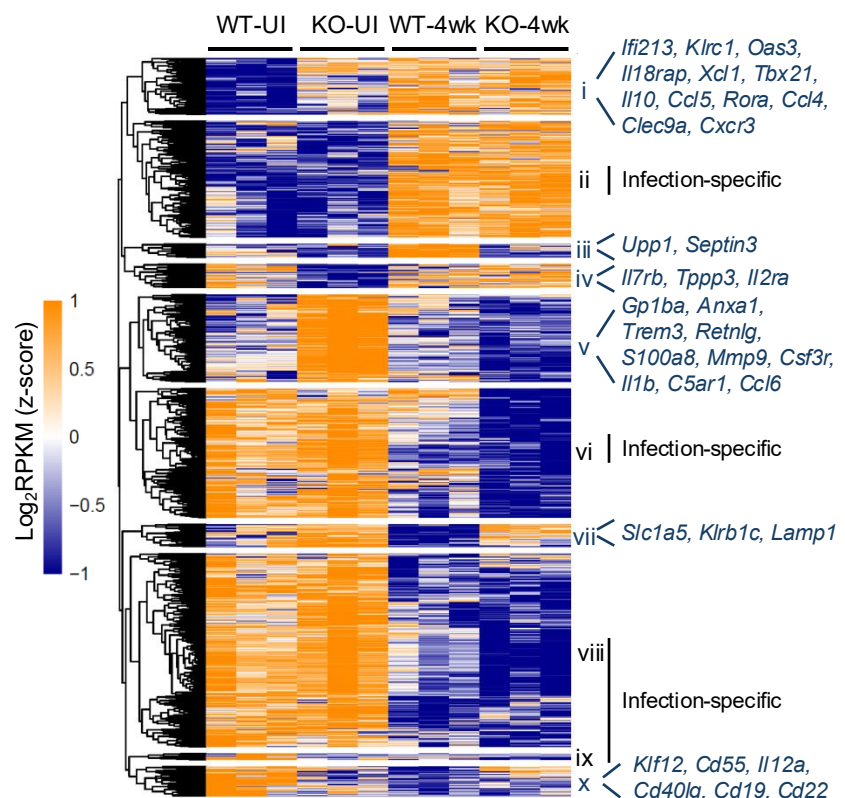
a.



c.

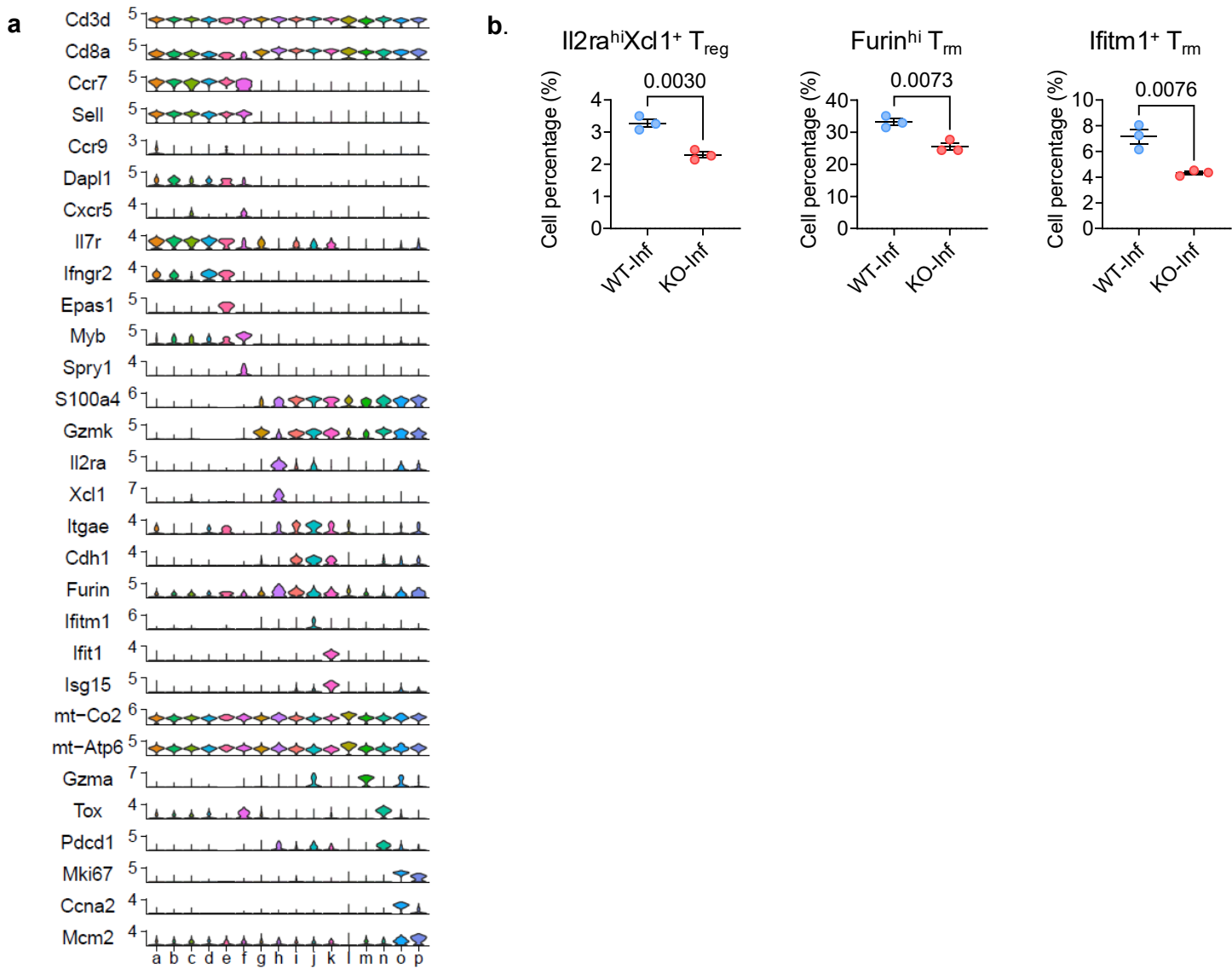


b.



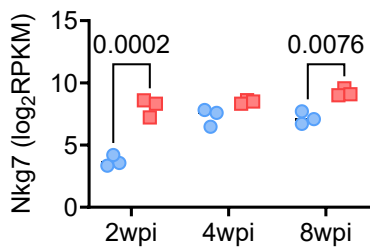
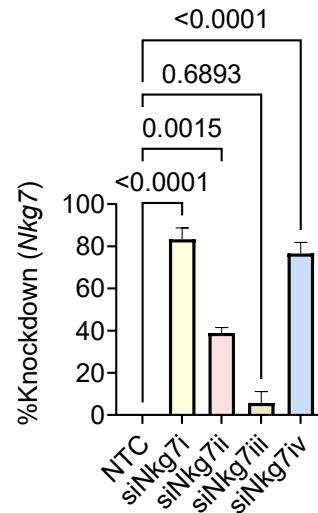
**Extended Data Fig. 2 Bulk RNA-seq of spleen CD8<sup>+</sup> T cells from uninfected and infected (4 wk) Nr4a1<sup>-/-</sup> and WT mice.**

**a**, Venn diagram showing the overlap of DEGs between 4 wk and uninfected (UI) CD8<sup>+</sup> T cells from WT and Nr4a1<sup>-/-</sup> mice. **b**, Heatmap of the union of 4 wk vs UI DEGs ( $n = 1,775$ ) identified in panel a. Log<sub>2</sub> RPKM values were z-score–normalized across samples. Genes were grouped into ten clusters (cluster i to x) using k-means clustering. Representative genes for clusters not classified as infection-specific are labeled on the right. **c**, GO biological processes among clusters i and v from panel b. Enriched biological processes include pathways related to cytokine-mediated signaling, natural-killer-like effector activity, leukocyte chemotaxis, and antibacterial defense. GO terms shown represent non-redundant categories with the lowest adjusted  $P$  values.



**Extended Data Fig. 3 Marker expression and subset frequencies from scRNA-seq data define CD8<sup>+</sup> T cell states in WT and *Nr4a1*<sup>-/-</sup> lungs.**

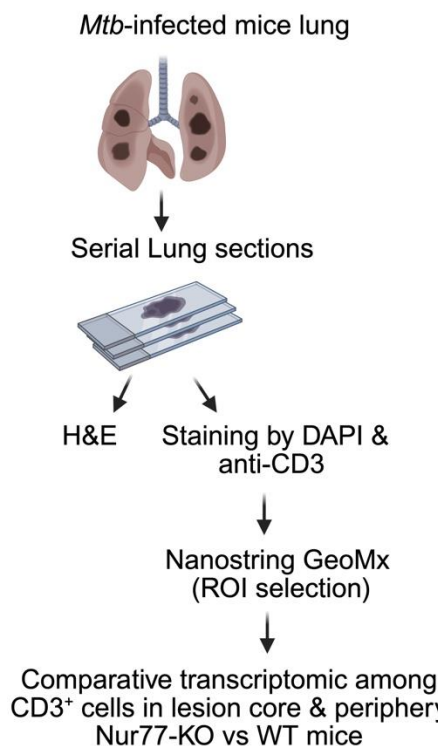
**a**, Expression of markers used to characterize CD8<sup>+</sup> T cell subtypes (see Methods for gene lists and normalization). **b**, Percentage of Il2ra<sup>hi</sup> Xcl1<sup>+</sup> T<sub>m</sub>, Furin<sup>hi</sup> T<sub>m</sub> and Ifitm1<sup>+</sup> T<sub>m</sub> in infected lungs (WT versus *Nr4a1*<sup>-/-</sup>); unpaired two-sided *t*-test; *P* values labeled.

**a.**Spleen - Bulk RNA seq  
CD8<sup>+</sup> T cells, WT vs KO**b.**

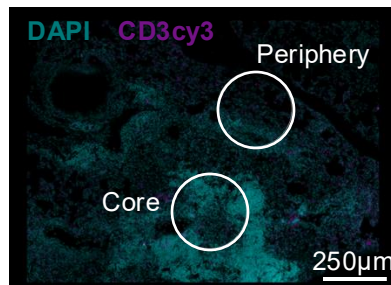
### Extended Data Fig. 4 *Nkg7* expression and its knockdown in CD8<sup>+</sup> T cells.

**a**, Bulk RNA-seq analysis showing *Nkg7* expression (log<sub>2</sub> RPKM) in splenic CD8<sup>+</sup> T cells from WT and *Nr4a1*<sup>-/-</sup> mice at 2, 4, and 8 wk of infection. *P* value, unpaired two-tailed *t* test. **b**, Efficiency of *Nkg7* knockdown in *Nr4a1*<sup>-/-</sup> CD8<sup>+</sup> T cells using four independent siRNAs, as measured by RT-qPCR 72 h post-transfection. Data mean  $\pm$  s.d.; one-way ANOVA.

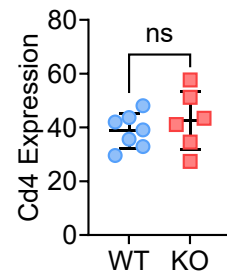
a.



b.



d.



e.

Pseudo-bulk DEGs in CD8<sup>+</sup> T cells, KO vs WT (1,407 genes), scRNA-seq data

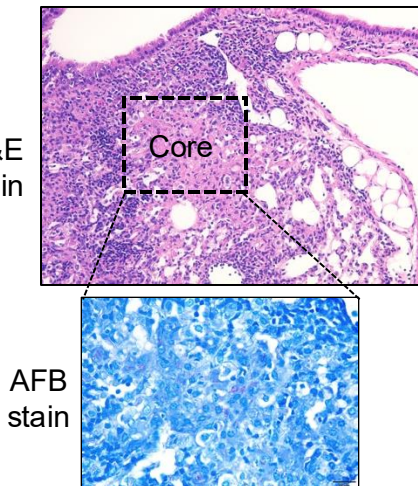
↓

Expression of these genes was evaluated in core and periphery CD3<sup>+</sup> T cells in the ROIs of GeoMx data

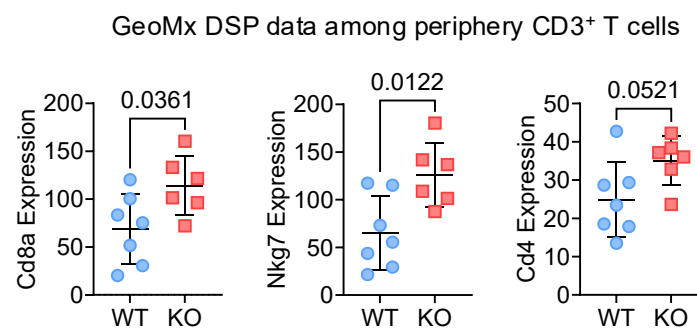
↓

Heatmap (Fig. 6h and Extended Fig. 5g)

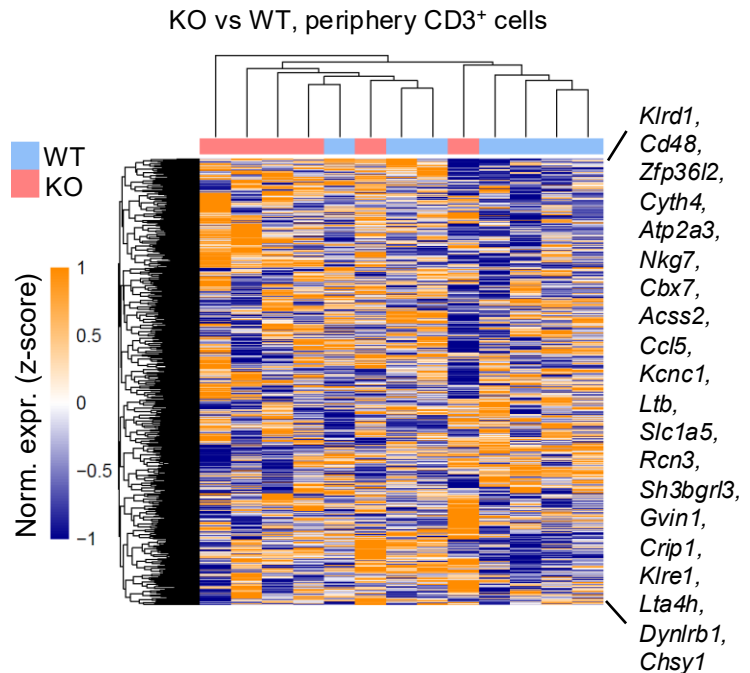
c.



f.

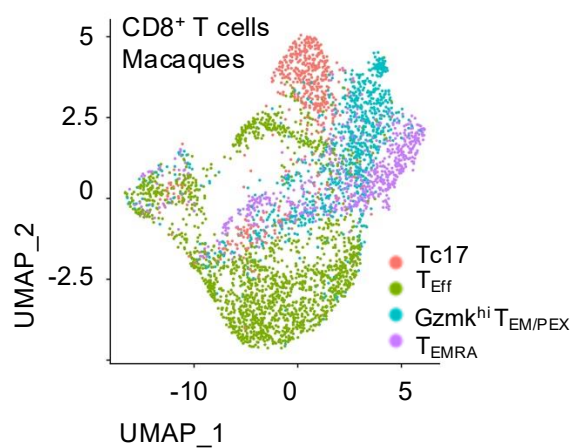
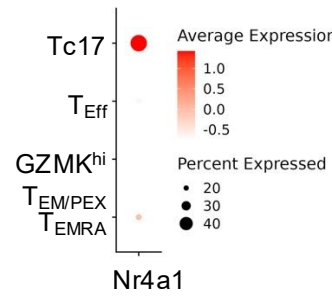
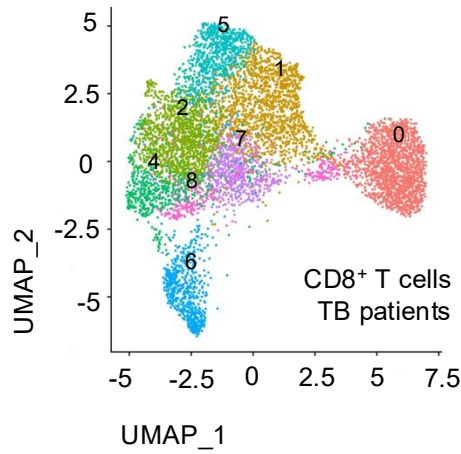
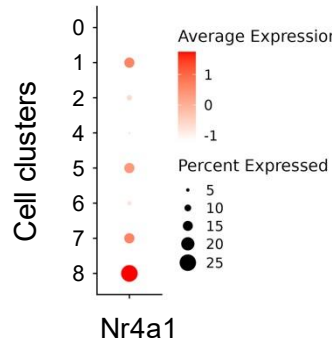


g.



## Extended Data Fig. 5 Spatial transcriptomic workflow and key readouts in *Mtb*-infected mice lungs.

**a**, Schematic of GeoMx spatial transcriptomics: serial lung sections; H&E and antibody staining (DAPI, CD3, CD11b) to guide ROI selection; comparative transcriptomics of CD3<sup>+</sup> and CD11b<sup>+</sup> cells in lesion core versus periphery, *Nr4a1*<sup>-/-</sup> versus WT. **b**, Immunofluorescence image showing ROIs in lesion core and periphery defined by DAPI and CD3 (Cy3) signal; scale bar, 250  $\mu$ m. **c**, Histology of infected lung sections: H&E (top) and acid-fast bacilli (AFB) stain (bottom). **d**, *Cd4* expression (normalized counts) in CD3<sup>+</sup> ROIs from WT and *Nr4a1*<sup>-/-</sup> (KO) lungs (*P* value, two-sided Mann–Whitney test). **e**, Schematic for the heat map generation by taking DEGs from CD8<sup>+</sup> T cell scRNA-seq data and finding their gene expression in periphery or core CD3<sup>+</sup> ROIs of spatial transcriptomic data. **f**, Expression levels of *Cd8a*, *Nkg7*, and *Cd4* in peripheral CD3<sup>+</sup> T cells from WT and *Nr4a1*<sup>-/-</sup> mice. *P* values, unpaired two-tailed *t* tests. **g**, Heatmap of the pseudo-bulk DEGs identified from total lung CD8<sup>+</sup> T cell scRNA-seq (Fig. 5b), evaluated in periphery CD3<sup>+</sup> ROIs from GeoMx spatial transcriptomics of *Mtb*-infected lungs. Distinct clustering of WT (blue) and *Nr4a1*<sup>-/-</sup> (red) samples was not observed among periphery CD3<sup>+</sup> ROIs. Representative cytotoxic and activation genes are indicated on right side. See Methods for DEG definition, normalization and clustering parameters.

**a.****b.****c.****d.**

**Extended Data Fig. 6** *Nr4a1* expression across lung CD8<sup>+</sup> T cell states in macaque and humans with TB, analysis of published scRNA-seq dataset.

**a**, UMAP of four lung CD8<sup>+</sup> T cell subtypes in *Mtb*-infected macaques. **b**, Bubble plot summarizing *Nr4a1* expression across the four lung CD8<sup>+</sup> T cell subtypes in **a** (dot size, percent expressing; color, average normalized expression). **c**, UMAP of eight CD8<sup>+</sup> T cell clusters in the lungs of active TB patients. **d**, Bubble plot summarizing *Nr4a1* expression across the eight clusters in **c** (dot size, percent expressing; color, average normalized expression). Dataset sources and accessions are listed in Methods.